

ATMOSPHERIC PRESSURE PLASMA JETS IN INERT GASES: ELECTRICAL, OPTICAL AND MASS SPECTROMETRY DIAGNOSIS

A.V. NASTUTA^{1,2}, I. TOPALA¹, V. POHOATA¹, I. MIHAILA¹, C. AGHEORGHIESEI¹,
N. DUMITRASCU¹

¹Iasi Plasma Advanced Research Center (IPARC), “Alexandru Ioan Cuza” University of Iasi,
Faculty of Physics, Blvd. Carol I No. 11, Iasi, 700506, Romania,

²Biomedical Sciences Department, Faculty of Medical Bioengineering,
Grigore T. Popa University of Medicine and Pharmacy Iasi, Str. M. Kogalniceanu, no. 9-13, Iasi,
700454, Romania

E-mail: andrei.nastuta@gmail.com

Received August 7, 2015

Abstract. Atmospheric pressure plasmas are continuously studied nowadays as promising tools for worldwide applications. Plasma jet sources are investigated by means of electrical, optical and mass spectrometry diagnosis. Experimental results revealed a strong influence of the discharge geometry and working gas upon plasma dynamics and active species production.

Key words: atmospheric pressure plasma jet, plasma bullets, electrical diagnosis, mass spectrometry.

1. INTRODUCTION

At the end of the last century started the challenge of novel experiments using atmospheric pressure plasmas for material processing in various forms, polymerization and even treatment of soft material, such as living cells / tissues / organs. An increasing interest was directed towards the **atmospheric pressure plasma jets (APPJ)** use for medical applications. Furthermore a continuously increasing number of reports on plasma based decontamination devices, wound healing, blood coagulation, treatment of dental cavities, induction of apoptosis for cancer cells and trials in cancer therapy, had been published by the scientific community [1–10].

Results obtained from the diagnosis of different atmospheric pressure plasma jets in argon and helium are reported in the present study. Using microsecond duration high voltage square pulses, the plasma is generated using the principle of a dielectric barrier discharge.

Electrical diagnosis was performed for monitoring and statistical analysis of plasma voltage and current recorded waveforms. Moreover global emitted light

from the plasma sources was monitored by time averaged techniques, such as emission spectroscopy and ultra-fast photography. Furthermore, mass spectrometry technique was applied in order to investigate the active species produced in the plasma jet volume. Combining the results retrieved from these diagnosis techniques, new insights on the plasma behavior and potential application can be revealed.

2. EXPERIMENTAL SETUP

Atmospheric pressure plasma jets are generated in helium and argon, using the dielectric barrier discharge (DBD) principles. The first plasma source used in these experiments consist of two copper tape electrodes fixed on the external surface of a quartz tube (Φ_{out} 6 mm, Φ_{in} 4 mm), and will be referred further on as **Jet-1** (Fig. 1). For the second plasma source a stainless steel hollow electrode (Φ_{out} 3 mm, Φ_{in} 2 mm) centered inside a quartz tube (Φ_{out} 6 mm, Φ_{in} 4 mm) and a copper tape electrode fixed on the external surface of a quartz tube are used, and will be referred further on as **Jet-2** (Fig. 1).

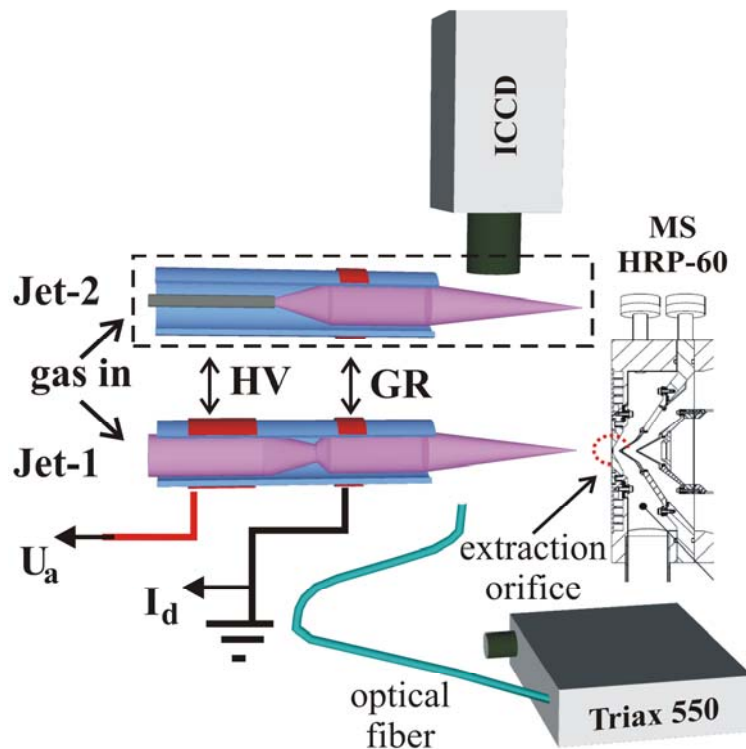


Fig. 1 – Sketch of the two plasma sources studied in this work.

In both configuration (**Jet-1** and **Jet-2**) the ground electrode is placed at 15 mm away from the quartz tube nozzle.

The working gas (He 4.6 and Ar 4.8, Messer) flows through the dielectric tube with a constant flow rate of 3 L/min (MKS 247 flowmeter), ensuring a laminar flow regime.

High voltage pulses, 6 kV amplitude and 40 μ s width, are applied on the power electrode, with 2 kHz repetition frequency, using a function generator (Tabor WW5064) and an amplifier (Trek PD07016). A high voltage probe (Tektronix 6015A) and a current probe (Pearson 6585) connected to a digital oscilloscope (Tektronix TDS 5034B) are used to record the voltage and current traces for further analysis.

Using a Triax 550 (Horiba Jobin Yvone, 600 lines/mm grating) spectrometer the optical emission spectra between 200–950 nm was acquired, *via* an optical fiber (400 μ m diameter).

For a better understanding of the plasma jet spatio-temporal dynamics we used the fast photography technique. An ICCD system (Hamamatsu C8484-05G camera coupled with an image intensifier C9546) was used to capture up to 30 ns exposure time images of the plasma jet [8, 11].

A HPR-60 MBMS mass spectrometer system (Hiden Analytical Ltd) was used for this study, with 2500 amu upper mass range [12]. Mass-to-charge ratio (m/z) spectra were collected, emphasizing the effect of surrounding ambient air on plasma active species. For these experimental studies plasma source **Jet-1** was placed at 3 mm away from the mass spectrometer entrance flange, directed to the extraction orifice (Fig. 1).

3. RESULTS AND DISCUSSIONS

3.1. ELECTRICAL DIAGNOSIS

The electrical signals, applied voltage and discharge current, for **Jet-1** and **Jet-2** plasma sources are shown in Fig. 2. For both **Jet-1** and **Jet-2** a double discharge behavior is observed, in helium and argon, characteristic for monopolar pulsed DBD discharges.

More precisely, as reported in the literature [13, 14], for the rising front of the applied voltage a current peak appears – mainly known as ‘primary discharge’; respectively, for the falling front of the applied voltage a second, with inversed polarity, current peak appears – known as ‘secondary discharge’.

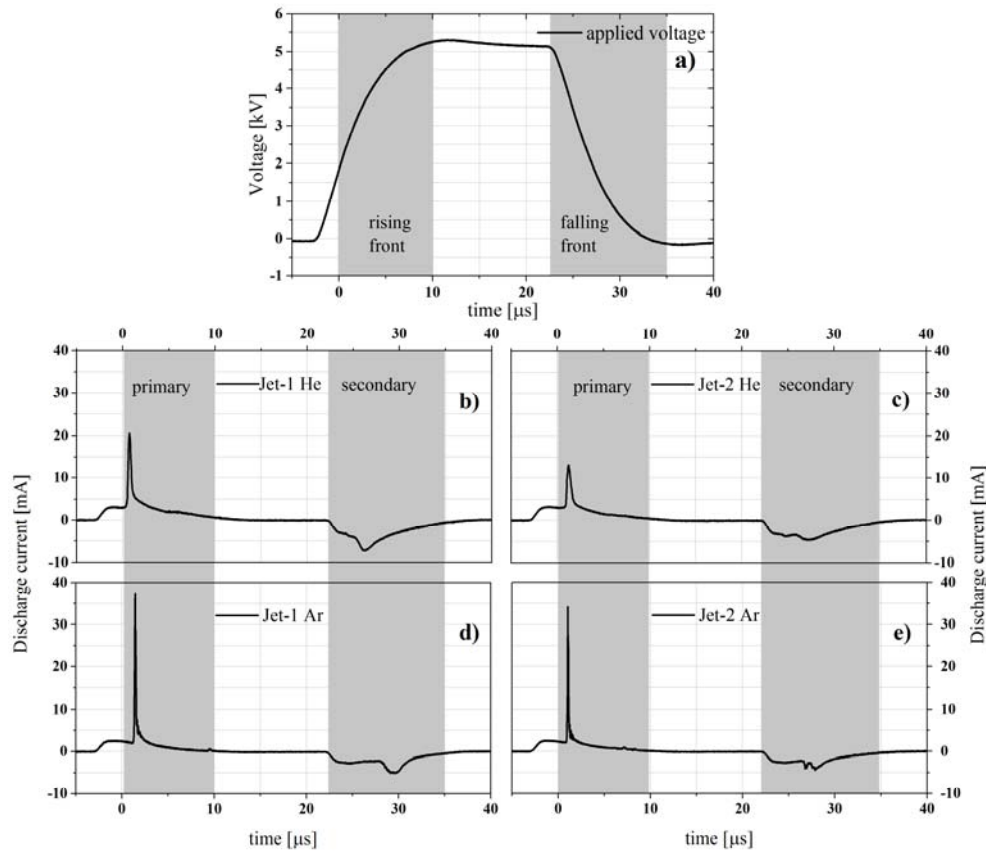


Fig. 2 – Typical waveforms of the applied voltage (a) and discharge current for **Jet-1** and **Jet-2** in He (b, c) and Ar (d, e).

From Fig. 2b–e it can be observed that the discharge current pulses are asymmetrical, both for He and Ar plasma jet. The current pulse following the rising voltage front is significantly higher in amplitude and narrow, while the current pulse in the falling front of the applied voltage is relatively weak and broadened. Discharge current varies from 13 mA (Jet-2 He) to 21 mA (Jet-1 He), and increases to 34 mA (Jet-2 Ar) respectively to 38 mA (Jet-1 Ar). Total charge (sum of integrated current peaks) varies from 46 nC (Jet-2 Ar) to 78 nC (Jet-1 He). The mean pulse energy was determined to be of ~ 6 W/s for plasma jet operating in He and ~ 3 W/s for plasma jet operating in Ar. These values are in conformity with those reported in risk assessments articles concerning the use of plasma in medicine [4–5].

3.2. OPTICAL EMISSION SPECTROSCOPY

Optical emission spectroscopy is a convenient technique for the identification and monitoring of several characteristics of the atmospheric pressure plasma jet in a noninvasive manner. An overview of the acquired emission spectrum of the plasma sources, at 2 mm away from the discharge tube, in the wavelength range 200–950 nm is shown in Fig. 3.

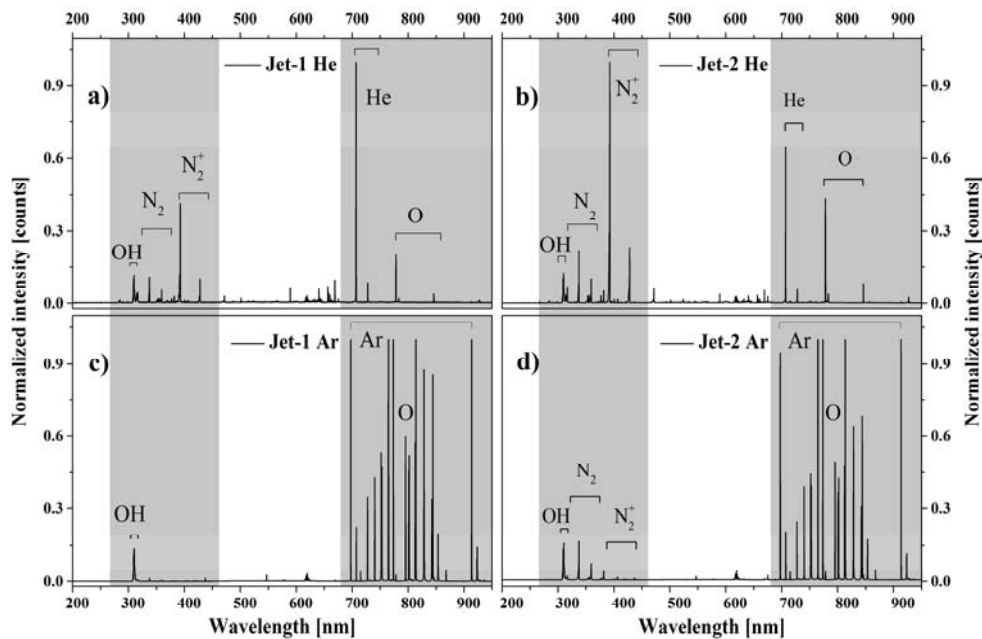


Fig. 3 – Emission spectrum for **Jet-1** and **Jet-2** plasma sources in He (a, b) and Ar (c, d).

It is well known that the emission spectra of this kind of atmospheric pressure plasma jet driven in helium or argon shows many excited and reactive species, such as oxygen reactive species (known as ROS) and nitrogen reactive species (known as RNS). Emission spectra of investigated plasma sources contain molecular bands assigned to hydroxyl radicals, neutral nitrogen molecules and nitrogen molecular ion, as observed in other previously reported studies on atmospheric pressure DBD sources [14, 15]. More precisely ROS are represented by the OH radical band (306–310 nm) and atomic oxygen lines (777 nm and 844 nm). These components (OH and O), which act as strong oxidizing species, makes the plasma jet suitable for biomedical applications [6, 16–20]. The RNS

were assigned to molecular nitrogen bands (N_2 : from 315 nm to 380 nm, 399 nm and 405 nm) and to nitrogen molecular ions bands (N_2^+ : from 391 nm to 470 nm). Atomic lines of the working gas were observed between 501 nm to 728 nm for helium jets (Fig. 3a–b) and starting from 697 nm to 923 nm for argon driven sources (Fig. 3c–d).

Estimated gas temperature, using the rotational band of OH radicals and LIFBASE simulation software [21], in these experiments was about 290 K, for He plasma jets, and up to 310 K, for Ar discharges.

Experimentally it can be observed a pronounced effect of both gas nature and electrode configuration upon plasma emitted light. Moreover it was found that the Jet-2 plasma source is more effective in RNS excitation / production than Jet-1, despite of the working gas. Nevertheless the differences in the light intensity of the N_2 and N_2^+ bands in Fig. 3 is based on the interaction processes between He atoms and nitrogen molecules (Penning effect) [6].

3.3. ULTRA-FAST PHOTOGRAPHY

Even though the plasma column that expand into air (for about 2 cm) seems continuously for both helium and argon, a different behavior at ns scale is revealed when using ultra-fast photography technique.

ICCD images for the plasma sources operating in He revealed a ‘bullet-like’ behavior for both discharges (Fig. 4). Helium plasma Jet-1 dynamics in open air had been reported elsewhere [8, 11]. When using Ar, plasma expands from the electrode region, through discharge tube and in open air, in a more continuum way. Moreover no ‘bullet-like’ structure was observed in Ar plasma jets studied. A ‘snake-like’ rotating plasma structure, moving along the inner surface of the discharge dielectric tube was recorded for both **Jet-1** and **Jet-2** sources (Fig. 4).

Using ICCD images, ‘plasma-bullet’ velocity for **Jet-1** plasma source, in He was found to range between 0.2 to 30×10^4 m/s, as reported previously in [6, 8, 11]. For the second plasma source, **Jet-2** in He (Fig. 4), the velocity value was found to range between 0.6 to 2×10^4 m/s. For the Ar plasma jet sources a mean velocity of the plasma was estimated to be up to 1.2×10^4 m/s, from the moment plasma passes the ground electrode and moves towards the dielectric tube exit (images from ‘200 ns’ to ‘1400 ns’ in Fig. 4 right column). Subsequently plasma remains for a longer time inside discharge tube, up to another 10 μ s (6 μ s more than in the He case).

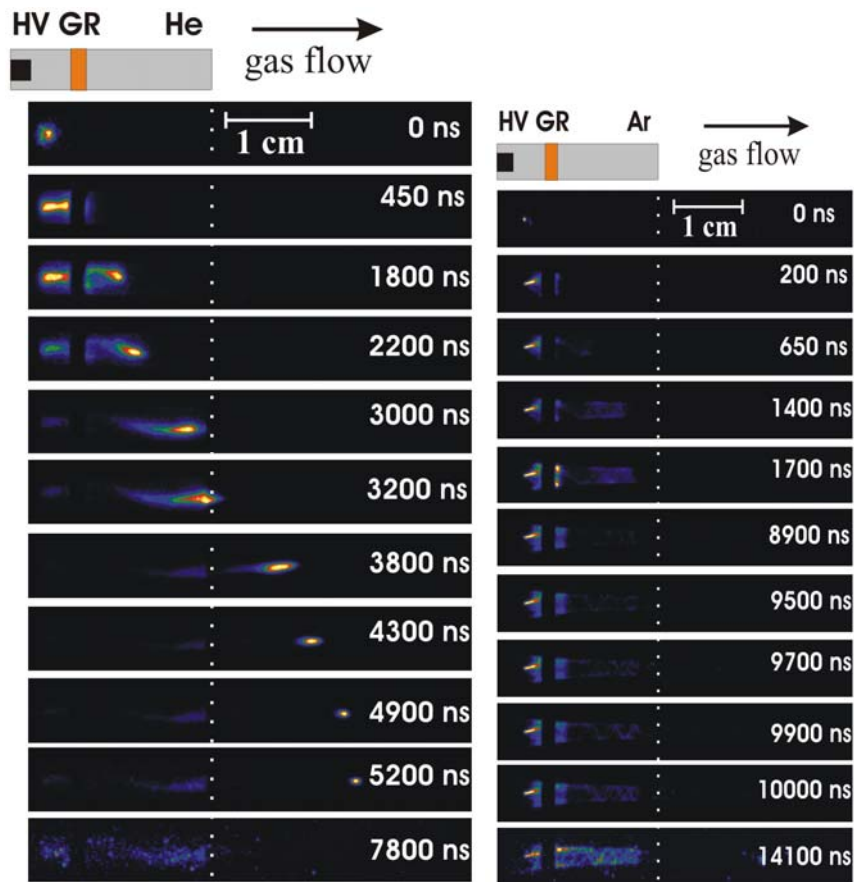


Fig. 4 – Typical ultra-fast images of Jet-2 in He (left column) and in Ar (right column). '0 ns' correspond to current pulse rising.

3.4. MASS SPECTROMETRY OF HE PLASMA SOURCE

In order to have an insight on plasma source chemistry mass spectrometry technique was used. Plasma effluent is composed of neutrals, ions, photons and it is sampled through spectrometer extraction orifice. In Fig. 5 are presented the mass spectra of the Jet-1 plasma source operating in He, at atmospheric pressure. Along residual gas analysis technique (RGA in Fig. 5a) also secondary ions mass spectrometry analysis technique (Sims in Fig. 5b – positive and c – negative ions) were used in order to characterize Jet-1 source. Due to experimental conditions (atmospheric pressure sampling) along plasma related species (helium or argon) impurities were also observed in the mass spectra (N_2 , N_2^+ , O_2 , NO and CO_2).

Moreover the presence of water clusters was recorded in mass-to-charge ratio spectra both for positive (Fig. 5b, *e.g.*: $\text{H}^+(\text{H}_2\text{O})$) and negative ions (Fig. 5c, *e.g.*: $\text{OH}^-(\text{H}_2\text{O})_n$, $\text{NO}_2^-(\text{H}_2\text{O})_3$). Similar results were reported recently for plasma jets by Oh, Benedikt and Große-Kreul *et al.* [12, 22–23] highlighting that in atmospheric pressure plasmas the formation of cluster ions is dominant.

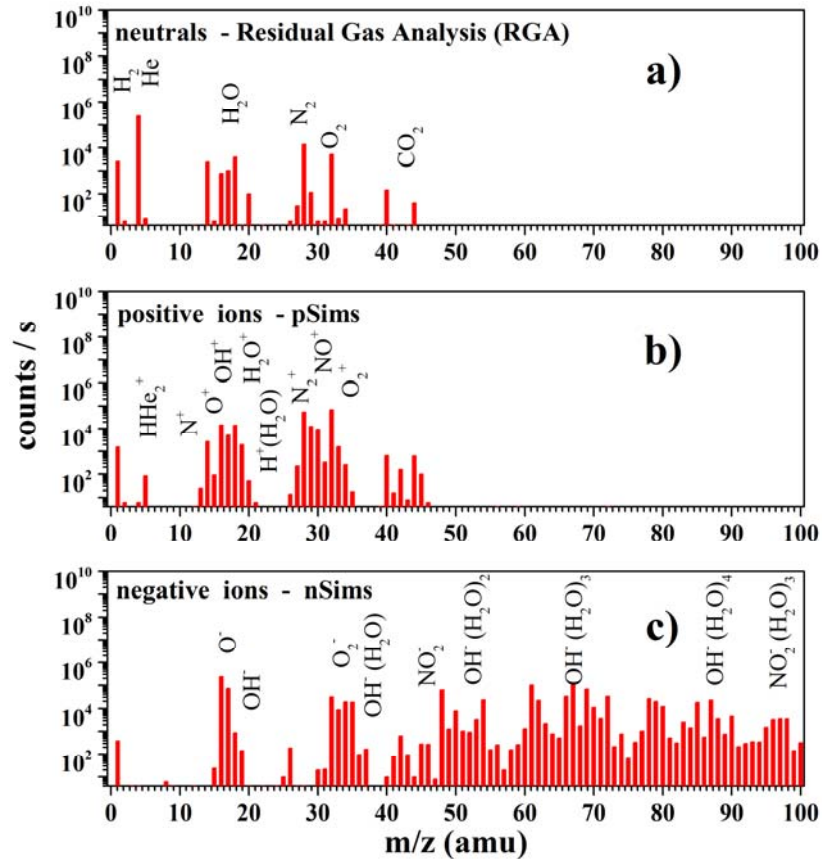


Fig. 5 – Mass spectra obtained using residual gas (a) and secondary ions mass spectrometry analysis (pSims – b and nSims – c) for Jet-1 plasma source, $Q_{\text{He}} = 3 \text{ L/min}$, $U_a = 6 \text{ kV}$.

As observed in the global emitted light spectra (Fig. 3), the studied discharges consist of helium and impurities from surrounding air. The presence of reactive species (ROS-RNS) in plasma volume, with great importance in Plasma Medicine field, was proven through MS measurement and it sustains the OES findings. This good correlation between these complementary techniques support the usage of studied plasma source in subsequent biomedical experiments. Following experiments combined with complementary electric and spectroscopic

diagnosis techniques may lead to a better understanding of mechanisms and dynamics of atmospheric plasma jets.

4. CONCLUSIONS

Two electrode configuration plasma sources were investigated by means of electrical, optical and mass spectrometry techniques, using He and Ar as working gas. A strong influence of both electrode geometry and working gas type upon plasma dynamics was found. Although from electrical diagnosis both Jet-1 and Jet-2 plasma sources seems equivalent, optical diagnosis revealed different plasma behaviour. ‘Bullet-like’ plasma structures were observed only when the discharge was operating in He. That was not the case when working in Ar. Using OES and MS techniques reactive species like OH, N₂, N₂⁺ and O could be recorded in the plasma volume. Plasma mechanisms are of great importance every time we have to apply a plasma based device in technology. Therefore in order to create or to use reliable and controllable plasma based devices more diagnosis techniques must be used in direct connection with the desired application.

Acknowledgments. This work was supported by the European Social Fund in Romania, Sectorial Operational Programme for Human Resources Development, grant POSDRU/159/1.5/S/133652. The POSCCE-O 2.2.1, SMIS-CSNR 13984-901, no. 257/28.09.2010, project CERNESIM, is gratefully acknowledged for the MS infrastructure used in this work.

REFERENCES

1. E. Stoffels, A. J. Flikweert, W. W. Stoffels, G. M. W. Kroesen, *Plasma Sources Sci. Technol.* **11**, 383 (2002).
2. G. Fridman, A. Shereshevsky, M. M. Jost, A. D. Brooks, A. Fridman, A. Gutsol, V. Vasilets, G. Friedman, *Plasma Chem. Plasma Proces.* **27**(2), 163 (2007).
3. G. Fridman, G. Friedman, A. Gutsol, A. B. Shekhter, V. N. Vasilets, A. Fridman, *Plasma Proces. Polym.* **5**(6), 503 (2008).
4. K. D. Weltmann, E. Kindel, T. von Woedtke, M. Hahnel, M. Stieber, R. Brandenburg, *Pure and Appl. Chem.* **82**(6), 1223 (2010).
5. G. Isbary, G. Morfill, H. U. Schmidt, M. Georgi, K. Ramrath, J. Heinlin, S. Karrer, M. Landthaler, T. Shimizu, B. Steffes, W. Bunk, R. Monetti, J. L. Zimmermann, R. Pompl, W. Stolz, *British J. Dermatol.* **163**(1), 78 (2010).
6. A. V. Nastuta, I. Topala, C. Grigoras, V. Pohoata, G. Popa, *J. Phys. D: Appl. Phys.* **44**, 105204 (2011).
7. A. Lupu, N. Georgescu, *Romanian Reports in Physics* **65**(1), 219–229 (2013).
8. A. V. Nastuta, V. Pohoata, I. Topala, *J. Appl. Phys.* **113**(18), 183302 (2013).
9. B.-G. Rusu, V. Pohoata, C. Ionita, R. Schrittwieser, N. Dumitrascu, *Rom. Journ. Phys* **61**, 518–526 (2016).
10. X. Deng, A. Yu Nikiforov, P. Vanraes, C. Leys, *Romanian Reports in Physics* **66**(4), 1088–1098 (2014).
11. A. V. Nastuta, I. Topala, G. Popa, *IEEE Trans. Plasma Sci.* **39**(11), 2310 (2011).

12. J.S. Oh, H. Furuta, A. Hatta, J.W. Bradley, J. J. Appl. Phys. **54**, 01AA03 (2015).
13. S. Liu, M. Neiger, J. Phys. D: Appl. Phys. **34**, 1632 (2001).
14. A. S. Chiper, G. B. Rusu, C. Vitelaru, I. Mihaila, G. Popa, Rom. Journ. Phys., **56**, 126–131 (2011)
15. D. Zaharie-Butucel, S. D. Anghel, Rom. Journ. Phys. **59**(7–8), 757–766 (2014).
16. B. Benstaali, P. Boubert, B. G. Cheron, A. Addou, J. L. Brisset, Plasma Chem. Plasma Proc. **22**, 553 (2002).
17. B. Benstaali, D. Moussa, A. Addou, J. L. Brisset, Eur. Phys. J. Appl. **4**, 171 (1998).
18. M. Laroussi, F. Leipold, Int. J. Mass. Spectrom. **233**, 81 (2004).
19. J. F. Kolb, A. A. H. Mohamed, R. O. Price, R. J. Swanson, A. Bowman, R. L. Chiavarini, M. Stacey, K. H. Schoenbach, Appl. Phys. Lett. **92**, 241501 (2008).
20. H. S. Uhm, J. P. Lim, S. Z. Li, Appl. Phys. Lett. **90**, 261501 (2007).
21. J. Luque, D.R. Crosley, *LIFBASE: Database and Spectral Simulation (version 1.5)*, SRI International Report, MP 99–009 (1999).
22. J. Benedikt, D. Ellerweg, S. Schneider, K. Rugner, R. Reuter, H. Kersten, T. Benter, J. Phys. D: Appl. Phys. **46**, 464017 (2013).
23. S. Große-Kreul, S. Hübner, S. Schneider, D. Ellerweg, A. von Keudell, S. Matejčík, J. Benedikt, Plasma Sources Sci. Technol. **24**, 044008 (2015).